Accurate Picometers for DC and Low-Frequency Displacement Measurement

J.R. Pratt[1] , D.T. Smith[1], and L.P. Howard[2]
[1]National Institute of Standards and Technology, Gaithersburg, MD 20899, USA
[2]Precera, Inc., Damascus, MD, 20872, USA

ABSTRACT
We have developed a fiber-optic interferometer optimized for best performance in the frequency range from DC to 1 kHz, with displacement linearity of 1 % over a range of ± 25 nm, and noise-limited resolution of 2 pm [1]. The interferometer uses a tunable infrared laser source (nominal 1550 nm wavelength) with high amplitude and wavelength stability, low spontaneous self-emission noise, high sideband suppression and a coherence control feature that broadens the laser linewidth and dramatically lowers the low-frequency noise in the system. The amplitude stability of the source, combined with the use of specially manufactured "bend-insensitive" fiber and all-spliced fiber construction, result in a robust homodyne interferometer system that achieves resolution of 40 fm·Hz$^{-1/2}$ above 20 Hz and approaches the shot-noise-limit of 20 fm·Hz$^{-1/2}$ at 1 kHz for an optical power of 10 μW, without the need for differential detection. Here we briefly review the design and construction of the interferometer, demonstrate its use for feedback stabilization of a probe displacement, and suggest a method to link the interferometer output to an absolute wavelength reference with an uncertainty on the order of 0.5% for displacements on the order of 100 pm.

FIBER INTERFEROMETER
The interferometer is shown schematically in Figure 1. The configuration is that of a simple fiber-optics-based, homodyne, single-detector interferometer; the components are in general the same as those described in Rugar et al. [2], with a few noteworthy modifications that are described in detail in Ref. [1]. Here, we highlight two important considerations that are required to achieve single-digit picometer resolution.

As described in Ref. [2], fairly broad spectrum, multi-mode diode laser sources are used for fiber interferometers because systems based on long-coherence-length light (e.g., narrow linewidth sources such as He-Ne lasers) were prone to spurious interference from stray reflections at optical interfaces. Such spurious interference is a known source of low-frequency noise. However, the remedy of using broad linewidth sources represents a compromise, since multi-mode diode lasers are prone to wavelength fluctuations that mimic a low-frequency displacement. In the work of Rugar *et al.* [2], this compromise manifested itself as linearly increasing noise as a function of fiber-to-reflector spacing, which led to the notion that for noise performance better than 10 pm, the fiber-to-reflector spacing must be kept below 5 μm, greatly limiting the applicability of the technique.

The system of Figure 1 solves this problem by employing a light source that exhibits both stable mean frequency and broad linewidth (e.g., "coherence control"). Using this latest generation light source the low-frequency performance of the interferomter is effectively decoupled from fiber-to-reflector spacing. Of course, several other critical design steps are employed to minimize low-frequency noise, which are beyond the scope of this paper (see Ref. [1] for a complete description). But as an example, consider that single-mode fibers tend to scatter light into the fiber cladding as they flex, resulting in bending-loss. Such intensity changes in a homodyne system are interpreted as displacements, and to minimize intensity fluctuations from fiber flexing we therefore resorted to a specially manufactured bend-insensitive fiber. We found that using this bend-insensitive, jacketless fiber significantly reduced the noise content in the 1 Hz to 20 Hz region when the interferometer signal was viewed on a spectrum analyzer; a simple 25 mm diameter mandrel-wrap test using an optical power meter showed a factor of 26 improvement over non-bend-insensitive fibers such as SMF-28.

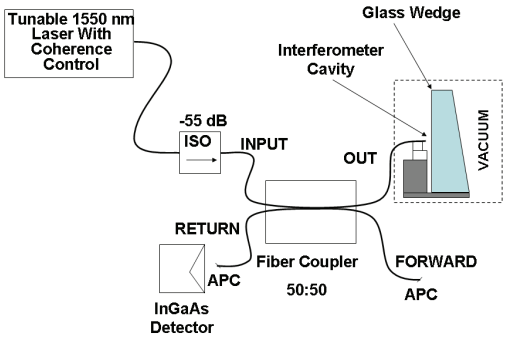

FIGURE 1. Schematic diagram of the fiber-optic interferometer showing the laser, optical isolator (ISO), evanescent wave coupler, single InGaAs detector and the interferometer cavity (note, APC means angle polished connector).

FEEDBACK STABILIZED PROBE

The feedback-stabilized probe instrument we consider here provides unprecedented stability and accurate dimensional measurement for the study of atomic point contacts by combining the positioning capabilities of a scanning tunneling microscope (STM) with the exceptional stability of a mechanically controlled break junction system [3]. The instrument is essentially an STM equipped with the fiber interferometer, which forms a cavity immediately adjacent to the probe (see Figure 2).

The probe and optical fiber assembly are positioned relative to a Au flat using two piezoelectric nanopositioners capable of both linear step motion over 5 mm and fine extension with sub-picometer control in vacuum at 4 K. One positioner moves the plate supporting the probe and fiber normal to the Au flat (the "*z*-axis" direction). The second positioner moves the Au flat perpendicular to the *z*-axis (the "*x*-axis" in Figure 2), allowing us to move to new positions on the Au flat as needed. The entire assembly is mounted to a base plate at the center of an inexpensive commercial cryogenic vacuum probe station chamber.

By using the interferometer output to control the *z*-axis positioner, the instrument can actively maintain a constant separation between the Au surface and the fiber end (and therefore the probe tip). The bandwidth of the servo-control loop (a commercially available analog proportional, integral, and derivative controller) is limited by the positioner dynamics to approximately 200 Hz, but this is sufficient for the cancellation of drift and low-frequency seismic and air-handling vibrations. For cavity lengths in the range 5 μm to 40 μm, we have determined that the interferometer resolution is noise-limited at 2 pm for quasistatic cavity measurements and at approximately 40 fm when low frequency (< 20 Hz) modulation is employed [1]. When changing the position set point in the control loop, cavity length changes as small as 5 pm can be clearly resolved; Figure 3 shows measured changes in cavity length resulting from set point changes.

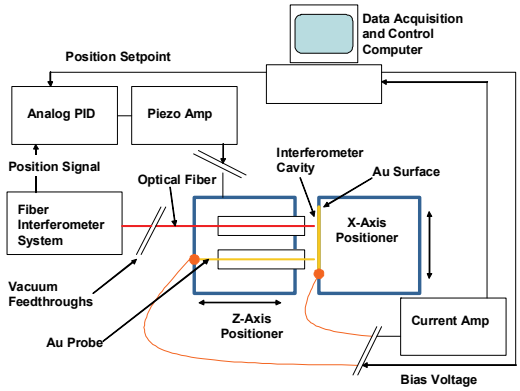

FIGURE 2. Probe system layout.

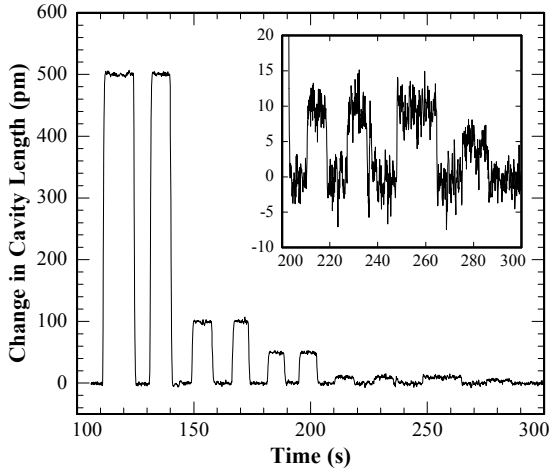

FIGURE 3. Observed changes in the interferometer cavity length as the servo control set point is changed. Set point changes as small as 5 pm produced well-defined changes in the cavity length. The data were taken in vacuum at 4 K.

DISPLACEMENT CALIBRATION

For a classical two-beam (TB) interferometer, interference produces sinusoidal "fringes" in both the transmitted and reflected light as the cavity length is varied. The normalized reflected intensity (for perfect visibility, discussed below) is given by [4]:

$$\frac{I_r(TB)}{I_p(TB)} = \frac{1}{2}\left[1-\cos\left(\frac{2\pi\Delta L}{\lambda}\right)\right] \qquad (1)$$

where the reflected intensity, I_r, at wavelength λ is normalized by the peak reflected intensity, I_p, and ΔL is the path length difference between the two beams. (Paths are assumed to be in vacuum, and have an index of refraction n = 1.000.) The sensitivity, S, of the system is then the change in detected intensity for a given change in ΔL, and is proportional to the derivative of Eq. 1. Maximum sensitivity occurs at the inflection, or quadrature, points on the fringes, where I_r/I_p = 0.5, and the phase angle $\varphi \equiv 2\pi\Delta L/\lambda = (2m+1)\pi/2$, for m an integer. Because in this work intensities are realized experimentally as voltages from photodetector amplifier circuits, we will switch notation such that V_{max} corresponds to Ip, where V_{max} is the detector output voltage at Ip, V_r corresponds to detector voltage for reflected intensity I_r, and $V_q = V_{max}/2$ is the detector voltage at quadrature. The sensitivity at quadrature, in terms of a detector voltage change for a given length change in ΔL is then given by:

$$S(TB) = \frac{\partial V_r}{\partial \Delta L} = \frac{2\pi V_q}{\lambda_q}, \qquad (2)$$

where λ_q is the wavelength at quadrature. *S(TB)* has units of V/m. This linearized sensitivity is valid only for small perturbations of the cavity from quadrature, and it should be clear that in this mode of operation the interferometer is intended for measuring displacements of a few tens of nanometers or less.

For a Fabry-Perot (FP) cavity formed between a pair of parallel air-glass or vacuum-glass interfaces the situation is more complicated. Here the equivalent to path length difference, ΔL, is now $2h$, where h is the cavity length. Normalized reflected power is given by the reflection coefficient $R = I_r/I_p$, and is approximately 0.04 for a single air/glass interface. Again, we take the case where the cavity is vacuum, with an index of refraction 1.000, and the cavity endfaces are glass. The reflected intensity from the cavity as a whole having interfaces with reflection coefficient R is no longer a sinusoidal function of h. Instead, it is given by the Airy function [5]:

$$\frac{V_r(FP)}{V_p(FP)} = \frac{(1+R)^2}{2}\left[\frac{1-\cos\left(\frac{4\pi}{\lambda}h\right)}{1+R^2-2R\cos\left(\frac{4\pi}{\lambda}h\right)}\right]. \qquad (3)$$

One consequence of this correction to the TB case is that the phase angle $\varphi = 4\pi h/\lambda$ at which V_r/V_p = 0.5 is no longer given by $(2n+1)\pi/2$ for integer n, but has shifted slightly. For R = 0.04, the phase angles where V_r/V_p = 0.5 become $\varphi = [(2n+1)\pi/2][1+(-1)^n 0.083]$.

As in the two-beam case above, the sensitivity of the interferometer to changes in h is determined from the derivative of normalized intensity. Taking the derivative of Eq. 3 with respect to h we find:

$$\left(\frac{\partial}{\partial h}\right)\frac{V_r(FP)}{V_p(FP)} = \frac{2\pi(1+R)^2}{\lambda}\left[\frac{(1-R)^2\sin\left(\frac{4\pi}{\lambda}h\right)}{\left[1+R^2-2R\cos\left(\frac{4\pi}{\lambda}h\right)\right]^2}\right]. \qquad (4)$$

Evaluating this expression with R = 0.04 for those phase angles φ where V_r/V_p = 0.5 [note when comparing *S(FP)* to *S(TB)* that ΔL corresponds to $2h$], we see that the sensitivity *S(FP)* of our FP interferometer at $V_q = V_{max}/2$ is:

$$S(FP) = 1.003 \cdot S(TB) = 1.003 \cdot \left(\frac{4\pi V_q}{\lambda_q}\right). \qquad (5)$$

It also is noted that the condition $V_q = V_{max}/2$ does not correspond exactly to the maximum possible sensitivity for a FP cavity, as determined from the maximum of Eq. 4, but for R small it is close to optimal, and serves as an

experimentally convenient and reproducible set-point. It is further noted than for the derivation of S(FP) above, it is assumed that the reflection coefficient R from both glass/air interfaces is the same, so that the detected output voltage V_{min} at a fringe minimum is very close to zero, as was the case in experiments.

The light source for our interferometer can be tuned stably and accurately over the wavelength range 1440 nm to 1640 nm. This tuning range enables two very convenient operational features. First, when we either have no control over the macroscopic cavity spacing, as for example in the case of measuring the deflection of a cantilever force sensor, or we choose not to change the cavity out of concerns for dimensional stability, we can still operate the interferometer at its maximum sensitivity by tuning λ, so long as the cavity is large enough to contain a V_q within the tuning range of the laser. Second, we can make an absolute determination of a fixed cavity length h by sweeping wavelength. Since maxima in reflected intensity occur when $4h/\lambda = 2m+1$ for both TB and FP fringes, assuming no phase shift at the interfaces (other than standard phase inversion), and minima occur when $4h/\lambda = 2m$, it follows directly that h can be calculated from the measured wavelength values λ_m and λ_{m+1} of two consecutive fringe maxima or minima:

$$h = \frac{1}{2}\frac{\lambda_m \lambda_{m+1}}{(\lambda_{m+1} - \lambda_m)} . \qquad (6)$$

For the tuning range of our laser, this means that we can make an absolute determination of cavities as small as h = 6 μm. If a consecutive maximum and minimum are used to calculate h, 3 μm cavities can be measured. Accuracy is limited by our ability to measure λ_m and λ_{m+1}. With curve fitting, wavelengths of maxima and minima can typically be determined within a range of ± 0.1 nm, permitting cavity length determination to better than one part in 1000.

Laser tunability also permits an independent check on the sensitivity given in Eq. 5 that can be linked to International System of Units (SI). The procedure is as follows. A cavity length and laser wavelength are selected such that the detector output is $V_q = V_{max}/2$ for wavelength λ. The cavity length h is then changed by a small amount ε, and the new output voltage ($V_q + \Delta V$) is recorded. The change ε in cavity size does not need to be known, provided that $\varepsilon \ll \lambda/2$. The laser wavelength is then tuned to a new wavelength ($\lambda + \Delta\lambda$) such that once again $V_q = V_{max}/2$. For a known cavity length h and fringe order m, it is then possible to relate ε to the actual cavity length change Δh and determine the sensitivity $\Delta V/\Delta h$. Subsequent displacement measurements made with such a system can thus be made traceable through SI-traceable laser wavelength calibration [6]. The procedure is straightforward, but assumes an unambiguous and monotonic relation between wavelength and measured intensity. At present, this procedure is limited in this set up to perhaps 0.5% relative uncertainty due to systematic fluctuations in the interferometer intensity (see Ref [1]).

CONCLUSIONS

We have developed an exceptionally stable experimental platform for the study of atomic scale contacts by placing an interferometer cavity directly adjacent to a probe. This allows us to close a servo loop around the junction separation with picometer stability, so as to remove thermal drift and low-frequency vibration artifacts. The system could greatly improve a number of contact, or near-contact, atomic-scale experiments, allowing direct and accurate measurement of the probe displacement with respect to the surface. In addition, future work will incorporate a second interferometer and a stiff elastic force sensor, such that direct measurements can be made of bond stiffness and breaking force. The interferometer design currently being used for measuring probe motion provides sufficient sensitivity for measuring the deflection of a stiff (> 100 N m^{-1}) cantilever force sensor.

REFERENCES

1. Smith, D.T., Pratt, J.R., Howard, L.P., Rev. Sci. Instrum., **80**, 035105 (2009).
2. D. Rugar, H.J. Mamin, and P. Guethner, Appl. Phys. Lett. **55**, 2588 (1989).
3. Smith, D.T. and Pratt, J.R., Applied Physics Letters, submitted, (2009).
4. M. Born and E. Wolf, *Principles of Optics*, Third Revised Edition, Pergamon Press (1964).
5. J.L. Santos, A.P. Leite, and D.A. Jackson, Applied Optics 31, 7361 (1992).
6. S.L. Gilbert, W.C. Swann and C.-M. Wang, NIST Special Publication 260-137, 2005 Edition.